Journal of Alloys and Compounds 507 (2010) 335–340

Contents lists available at ScienceDirect

Journal of Alloys and Compounds

journal homepage: www.elsevier.com/locate/jallcom

Review

# Crystal growth and thermal properties of single crystal monoclinic NdCOB ($NdCa_4O(BO_3)_3$)

Cong Zhang[a], Zhen Li[a], Hengjiang Cong[a], Jiyang Wang[a,*], Huaijin Zhang[a], R.I. Boughton[b]

[a] State Key Laboratory of Crystal Materials, Shandong University, Jinan 250100, PR China
[b] Department of Physics and Astronomy, Bowling Green State University, Bowling Green, OH 43403, USA

ARTICLE INFO

*Article history:*
Received 18 March 2010
Received in revised form 21 July 2010
Accepted 27 July 2010
Available online 4 August 2010

*PACS:*
81.10.Fq
61.50.–f
66.30.Xj
65.40.De

*Keywords:*
Characterization
Crystal structure
Czochralski method
Single crystal growth
Borates
Nonlinear optic materials

ABSTRACT

A new member of the $RECa_4O(BO_3)_3$ crystal system, a neodymium calcium oxoborate [$NdCa_4O(BO_3)_3$, abbreviated as NdCOB] single crystal, with dimensions of 30 mm in diameter and 25 mm in length, has been grown along the crystallographic *b*-axis by the Czochralski method. X-ray powder diffraction results show that the as-grown NdCOB crystal, is of a single phase and belongs to the monoclinic system with space group Cm. The measurement and calculation of the symmetric second-rank tensors representing thermal properties of the monoclinic crystal, including thermal expansion and conductivity, are described in detail in this paper. The principal coefficients of thermal expansion of the as-grown NdCOB crystal are 6.75189, 6.3727 and 12.13381 ($10^{-6}\,K^{-1}$), respectively, over the temperature range of 303.15–768.15 K. The specific heat of the crystal is 0.65775 $J\,g^{-1}\,K^{-1}$ at 300.23 K. The principal thermal conductivity parameters are 1.9642, 1.8885 and 2.0374 $W\,m^{-1}\,K^{-1}$, respectively, at 303.35 K.


**Contents**



* Corresponding author. Tel.: +86 531883664340; fax: +86 53188564963.
*E-mail address:* jywang@icm.sdu.edu.cn (J. Wang).

0925-8388/$ – see front matter © 2010 Published by Elsevier B.V.
doi:10.1016/j.jallcom.2010.07.174

## 1. Introduction

In recent years, excellent nonlinear optical properties of $ReCa_4O(BO_3)_3$ crystals (R, rare-earth elements; ReCOB) (Re = Pr, Nd, Sm, Eu, Dy, Ho, Er) have been reported by researchers. The low symmetry of the crystal makes ReCOB crystals prime candidates for exhibiting NLO effects. When the rare-earth ions are replaced by a laser active ion, such as Nd or Yb, these crystals can perform both as lasers and frequency doublers. Thus, ReCOB crystals have been developed as host materials with the goal of obtaining a specific crystal that possesses self-frequency doubling properties (SFD) [1].

In 1992, Norrestam et al. [2] synthesized a new family of rare-earth oxoborates $ReCa_4O(BO_3)_3$ (Re = $La^{3+}$, $Nd^{3+}$, $Sm^{3+}$, $Gd^{3+}$, $Er^{3+}$, $Y^{3+}$). In 1996, Aka et al. [3] reported a study on $GdCa_4O(BO_3)_3$ (GdCOB) as a new nonlinear crystal. GdCOB was considered as a suitable nonlinear crystal that could be grown using the Czochralski method to obtain large dimensions and high optical quality. Later, Iwai et al. [4] reported in detail on $ReCa_4O(BO_3)_3$ (Re = Y or Gd) as another promising nonlinear crystal The NLO properties of GdCOB, YCOB and KDP were compared, and it was pointed out that YCOB has a larger nonlinear coefficient, greater temperature stability and dual refractive indices, properties which are useful for phase matching. At CLEO'98, Yoshimura et al. [5] reported the achievement of 1.064 μm second harmonic generation (SHG) and third harmonic generation (THG) as well.

$NdCa_4O(BO_3)_3$ (NdCOB) is one member of the rare-earth calcium oxoborates. In this crystal, the activated ion $Nd^{3+}$ is a stoichiometric component of the crystal instead of a dopant as in most other laser crystals. One of the prominent self-activated laser crystals is $NdAl_3(BO_3)_4$ (NAB), which is known to contain the highest concentration of $Nd^{3+}$ ions ($5.73 \times 10^{21}$ $cm^{-3}$) and possesses low concentration quenching, high gain, and good physical and chemical properties [6]. In a similar way as NAB, we expect NdCOB to be a self-activated laser crystal that possesses good optical and laser properties. There has not been much research carried out on NdCOB. There are only a few published reports on NdCOB mainly pertaining to its growth and piezoelectricity [7–10].

For a laser crystal, the thermal properties are some of the important factors governing its application, especially for high Nd-concentration crystals. A number of deleterious thermal problems can occur because of the heat generated during lasing, such as thermal focusing, stress-induced birefringence, stress-induced biaxial focusing, concentration quenching effects, and even cracking [11]. Thus, it is essential to determine the thermal properties of NdCOB, including the thermal expansion and thermal conductivity. These parameters will help characterize the heat transport and the degree of cooling efficiency in this material.

NdCOB, together with $Nd_xY_{1-x}COB$ crystals of different $Nd^{3+}$ concentration have been grown using the pulling (Czochralski) method. The specific heat measurements were carried out with a differential scanning calorimeter using a simultaneous thermal analyzer (NETZSCH LFA 447 Nanoflash). The thermal expansion of NdCOB was measured over the temperature range of 303.15–769.15 K using a thermal dilatometer (NETZSCH DIL 402C). The thermal diffusion coefficient of NdCOB was measured by the laser flash method using a laser flash apparatus (NETZSCH LFA 447 Nanoflash) over the temperature range of 303.15–562.15 K. In this paper, the thermal properties of NdCOB are discussed.

## 2. Experiments and results

### 2.1. Crystal growth and phase identification

Single crystals were grown by the traditional Czochralski technique, as NdCOB belongs to the calcium–rare-earth (R) oxoborate family. Initially, polycrystalline NdCOB was synthesized at 900 °C and 1150 °C, respectively, using $Nd_2O_3$, $CaCO_3$ and 4N pure $H_3BO_3$ in stoichiometric proportions in the following reaction:

$$Nd_2O_3 + 8CaCO_3 + 6H_3BO_3 \rightarrow 2NdCa_4O(BO_3)_3 + 8CO_2\uparrow + 9H_2O\uparrow$$

Because of the volatility of $H_3BO_3$, we added more $H_3BO_3$ than the calculated amount of about 1% of the total weight of the material. The polycrystalline NdCOB was heated at 900 °C in order to decompose the $CaCO_3$ and $H_3BO_3$, and to eliminate the effects of $CO_2$ and other vapors. Next, the polycrystalline NdCOB was pressed into bulk form under pressure, with the goal that the solid-state reaction can be carried out completely. After being pressed, the polycrystalline bulk material was heated at 1150 °C to promote the solid-state reaction.

The polycrystalline bulk material was then shifted to an iridium crucible for the growth of the NdCOB crystal. It was heated in a 2.5 kHz intermediate frequency furnace. Using a *b*-oriented YCOB single crystal bar as seed, a pulling rate of 0.2–0.3 mm/h, and a rotation rate of 15 rpm were adopted. The pulling rate was adjusted a bit during different periods of the crystal growth—decreasing with the increase in diameter to 0.1 mm/h by the time when the diameters were equal. The low pulling rate contributes to the high quality of the crystal. After the growth process was completed, the crystal was cooled to room temperature at a rate of 15 °C $h^{-1}$. The process of annealing, which was performed in air, was undertaken to decrease internal stress.

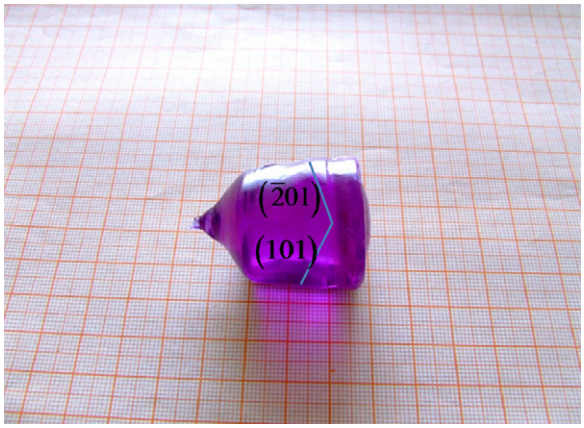


**Fig. 1.** NdCOB grown through the Czochralski method.

Fig. 1 shows the crystal as grown, with a diameter of 30 mm and length of 25 mm in the region where the diameter is constant. Because of the high $Nd^{3+}$ density, the crystal had a dark violet color. The high absorbance of $Nd^{3+}$ leads to almost total opacity. It can be seen that the crystal has two sets of natural facets parallel to the *b*-axis; they are identified as the $(\bar{2}\,0\,1)$ and $(1\,0\,1)$ planes.

Fig. 2 compares the XRPD patterns of the as-grown NdCOB crystal boule and the standard JCPDF data for this crystal (International Centre for Diffraction Data, Newton Square, PA, USA). It can be seen that the XRPD peak position of the crystal is in good agreement with the standard value. The slight difference in the peak intensities can be ascribed to a minor misorientation of the sample. The XRPD pattern is similar to that of YCOB [12], which indicates that NdCOB belongs to the monoclinic system

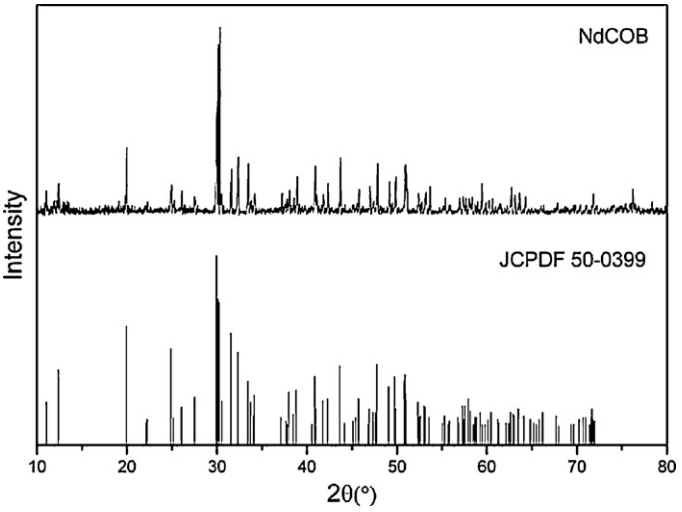


**Fig. 2.** XRPD patterns of the as-grown NdCOB crystal compared to standard data.

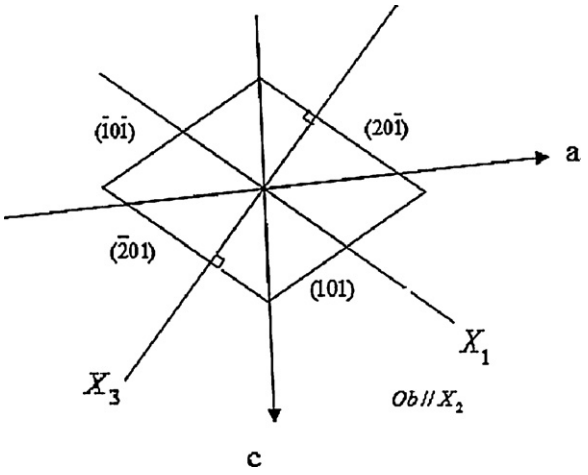


**Fig. 3.** Schematic diagram of the cross-section of the *b*-axis-grown crystal.

with space group Cm. Lattice constants at room temperature were determined to be: $a = 0.813$, $b = 1.606$, and $c = 0.359$ nm, and $\beta = 101.4^\circ$ [13].

### 2.2. Density measurements

The density of NdCOB was measured using the flotation method on a scale at room temperature, 299.15 K. Two random samples cut from the original crystal were used for the measurement with a resulting value of 3.62073 g cm$^{-3}$ at 299.15 K.

### 2.3. Thermal expansion measurements

The thermal expansion of a crystal has a great influence on crystal growth and on possible applications [14]. The thermal expansion was measured using a thermal dilatometer (NETZSCH DIL 402C) over the range of 303.15–769.15 K. During thermal expansion measurements, a constant rate of 5 K min$^{-1}$ was taken from 303.15 to 769.15 K to heat the crystal samples, and the results were recorded.

### 2.4. Specific heat measurement

For laser crystals, the damage threshold and therefore possible laser applications can be greatly influenced by the magnitude of the specific heat [15]. A slice of the as-grown NdCOB crystal, weighing 8.72 mg, was used as the sample. A small Pt–Rh crucible was used as a container to hold the sample. It was heated from 293.15 to 573.15 K at a constant rate of 5.00 K min$^{-1}$.

### 2.5. Thermal diffusion coefficient measurements

Measurements were made over the range of 303.15–562.15 K using five square (6 mm × 6 mm × 2 mm) crystal slices coated with graphite on both sides. The slices were cut along the same directions as those adopted in the thermal expansion measurements. The results will be discussed in the following section.

## 3. Discussion

### 3.1. Crystal orientation for thermal properties measurements

Crystal orientation is important in all physical measurements on crystals because the precise orientation in a low-symmetry monoclinic system has great influence in affecting the values of anisotropic physical properties. Since the crystallographic axes (*a*, *b*, *c*) in the low-symmetry monoclinic system are not mutually orthogonal, it is important to be attentive to the orientation of the crystallographic axes (*a*, *b*, *c*) with respect to the reference axes ($X_1$, $X_2$, $X_3$) of the conventional coequal system. Fig. 3 presents a schematic diagram of the cross-section of the NdCOB crystal, which is a parallelogram formed by the natural facets $(\bar{2}\,0\,1)$, $(2\,0\,\bar{1})$, $(1\,0\,1)$ and $(\bar{1}\,0\,\bar{1})$. It is typical of monoclinic crystals as discussed by Ye and Chai [16]. In Fig. 3, the crystallographic axes (*a*, *b*, *c*) and the reference axes ($X_1$, $X_2$, $X_3$) are determined by the right-hand rule. The reference axes $X_2$ and $X_3$ are perpendicular to the $(0\,1\,0)$ and $(\bar{2}\,0\,1)$ crystallographic planes, and $X_1$ is perpendicular to $X_3$. The angular

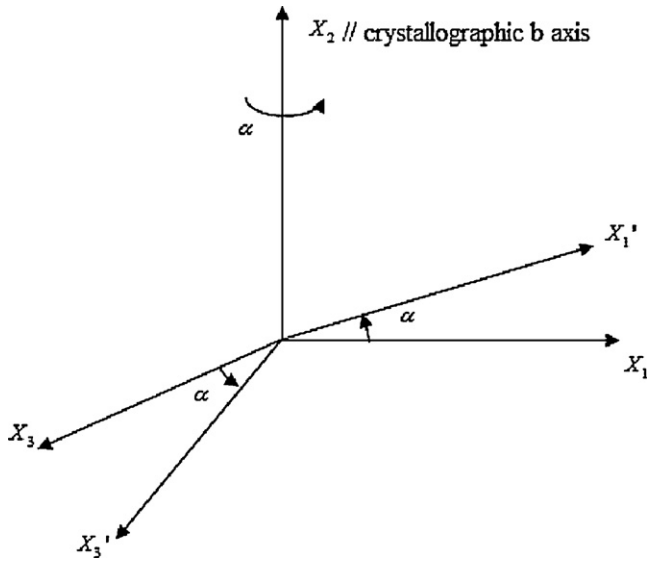


**Fig. 4.** Reference coordinates for monoclinic crystal system.

relationships between the crystallographic axes (*a*, *b*, *c*), reference axes ($X_1$, $X_2$, $X_3$) and natural facets were calculated using the unit-cell parameters of the NdCOB crystal: $X_2 || b$, $(X_1, a) = 25.4410^\circ$ and $(X_3, c) = 14.0696^\circ$.

Using the ($X_1$, $X_2$, $X_3$) coordinates as a basis, crystal samples were easily cut from the NdCOB single crystal and then used to carry out thermal expansion and thermal diffusion measurements.

### 3.2. Symmetric second-rank tensor measurement for monoclinic crystal

NdCOB belongs to the monoclinic system with m point-group symmetry. Both the thermal expansion coefficient and thermal conductivity are symmetric second-rank tensors that can be easily represented in the form of a $3 \times 3$ matrix $[T_{ij}]$ $(i, j = 1–3)$. In the monoclinic system, the crystallographic *b*-axis is one of the principal axes of the symmetric second-rank tensor $[T_{ij}]$, so $[T_{ij}]$ referred to the ($X_1$, $X_2$, $X_3$) coordinate system shown in Fig. 3 can be represented as [17].

$$\begin{pmatrix} T_{11} & 0 & T_{31} \\ 0 & T_{22} & 0 \\ T_{31} & 0 & T_{33} \end{pmatrix}$$

The values of the components $T_{11}$, $T_{22}$, $T_{33}$ can be determined directly from our measurements along $OX_1$, $OX_2$, and $OX_3$. The component $T_{31}$ can be calculated by means of the Mohr circle construction.

In Fig. 4 the axes $OX_1'$ and $OX_3'$ are obtained by rotating the original reference axes $OX_1$ and $OX_3$ counterclockwise around $OX_2$ through an angle $\alpha$ (negative if the rotation is clockwise). The transformation matrix is presented as follows:

$$\begin{pmatrix} \cos\alpha & 0 & -\sin\alpha \\ 0 & 1 & 0 \\ \sin\alpha & 0 & \cos\alpha \end{pmatrix}$$

Related to the new coordinate system, the symmetric second-rank tensor $[T_{ij}']$ can be represented as

$$\begin{pmatrix} T_{11}' & 0 & T_{31}' \\ 0 & T_{22}' & 0 \\ T_{31}' & 0 & T_{33}' \end{pmatrix}$$

In the same way as with the original coordinate system, the values of the components of $[T_{ij}]$ can be directly obtained from measurements along the $OX'_1$, $OX'_2$ and $OX'_3$ directions. Corresponding to the transformation law for second-rank tensors, we can determine the relationship between the components in the original coordinate system and in the new one:

$$T'_{11} = T_{11}\ \cos^2\alpha + T_{33}\ \sin^2\alpha - T_{31}\ \sin 2\alpha \quad (1)$$

$$T'_{22} = T_{22} \quad (2)$$

$$T'_{33} = T_{11}\ \sin^2\alpha + T_{33}\ \cos^2\alpha + T_{31}\ \sin 2\alpha \quad (3)$$

$$T'_{31} = (T_{11} - T_{33})\frac{\sin\ 2\alpha}{2} + T_{31}\ \cos 2\alpha \quad (4)$$

Because of the error inherent in the experiment, the values of $T_{31}$, obtained from Eqs. (1) and (2), are not always quite in accord with each other. In order to reduce the error, we used the least-squares method as follows [17,18]:

Because there are a total of four groups of experimental data, we introduce the following matrix:

$$\Theta = \begin{pmatrix} \sin^2\theta_1 & \sin 2\theta_1 & \cos^2\theta_1 \\ \sin^2\theta_2 & \sin 2\theta_2 & \cos^2\theta_2 \\ \sin^2\theta_3 & \sin 2\theta_3 & \cos^2\theta_3 \\ \sin^2\theta_4 & \sin 2\theta_4 & \cos^2\theta_4 \end{pmatrix} = \begin{pmatrix} 0.05908 & -0.47162 & 0.9409 \\ 0.9409 & 0.47162 & 0.059098 \\ 0.26419 & 0.8818 & 0.7358 \\ 0.7358 & -0.8818 & 0.26419 \end{pmatrix} \quad (5)$$

The angle $\theta_n$ represents the angle of rotation counterclockwise from the $c$ crystallographic direction. Specifically in this experiment, $\theta_n$ takes on the values −14.0696, 75.9304, 30.9304 and 120.9304 for $n$ = 1–4, respectively, representing directions along $OX_3$, $OX_1$, $OX'_3$, and $OX'_1$. The transformation matrix takes the form

$$R = \left(\Theta_T\Theta\right)^{-1}\Theta_T = \begin{pmatrix} -0.1909 & 0.6909 & 0.0142 & 0.4858 \\ -0.2358 & 0.2358 & 0.4409 & -0.4409 \\ 0.6909 & -0.1909 & 0.4858 & 0.0142 \end{pmatrix} \quad (6)$$

where $\Theta_T$ is the transpose of $\Theta$. We can then obtain all the components, $T_{11}$, $T_{33}$ and $T_{31}$ from the following equation:

$$\begin{pmatrix} T_{11} \\ T_{31} \\ T_{33} \end{pmatrix} = R \begin{pmatrix} X_3 \\ X_1 \\ X'_3 \\ X'_1 \end{pmatrix} \quad (7)$$

Thus we can use these values of $T_{11}$, $T_{31}$ and $T_{33}$ instead of the original elements to construct the symmetric second-rank tensor with only minor errors.

The next step is to determine the orientation of the principal axes $(X_I, X_{II}, X_{III})$ and the values of the principal components of $[T_{ij}]$. The symmetric second-rank tensor $[T_{ij}]$ referred to its principal axes $(X_I, X_{II}, X_{III})$ can be represented as

$$\begin{pmatrix} T_I & 0 & 0 \\ 0 & T_{II} & 0 \\ 0 & 0 & T_{III} \end{pmatrix} \quad (8)$$

Observing the matrix in the new coordinate system after rotation, we recognize that if the value of $T'_{31}$ equals zero, the form of the matrix would be diagonal. So the orientation of the principal axes can be determined by setting Eq. (4) to equal zero, which gives the angle between the principal axes $(X_I, X_{II}, X_{III})$ and the reference axes $(X_1, X_2, X_3)$ as expressed by the following equation:

$$\theta = \frac{1}{2}\arctan\left(\frac{2T_{31}}{T_{33} - T_{31}}\right) \quad (9)$$

Accordingly, the components $[T_I, T_{II}, T_{III}]$ of the principal axes $(X_I, X_{II}, X_{III})$ can be calculated by substituting $\theta$ for $\alpha$ in Eqs. (1) and (3).

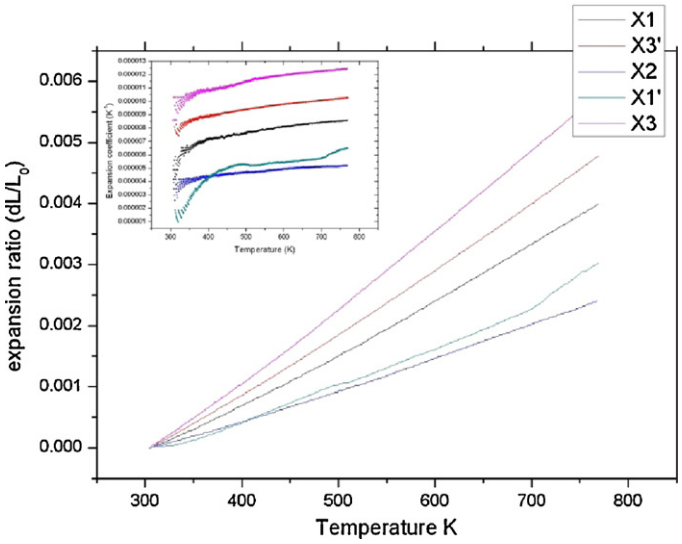


**Fig. 5.** Expansion ratio $\Delta L/L_0$ and coefficient $\alpha$ of NdCOB measured along $OX_1$, $OX_2$, $OX_3$, $OX'_1$ and $OX'_3$ orientations in the reference frame.

### 3.3. Thermal expansion of NdCOB crystal

Two rectangular crystal samples were cut from the NdCOB crystal. One sample was cut along the reference axes $(X_1, X_2, X_3)$ as shown in Fig. 3, and the other was cut with a counterclockwise angle $\alpha = 45^\circ$ along the reference axes $(X'_1, X'_2, X'_3)$ as shown in Fig. 4. The thermal expansion ratio versus temperature curves, measured along the $OX_1$, $OX_2$, $OX_3$, $OX'_1$ and $OX'_3$ directions, are shown as solid lines in Fig. 5.

Clearly, the thermal expansion ratio curves are nearly linear over the entire measurement range from 303.15 to 768.15 K. The average linear thermal expansion coefficient for the $OX_1$, $OX_2$, $OX_3$, $OX'_1$ and $OX'_3$ directions can be calculated according to the following formula [19]:

$$\overline{\alpha}(T_0 \rightarrow T) = \frac{\Delta L}{L_0}\frac{1}{\Delta T} \quad (10)$$

where $\overline{\alpha}(T_0 \rightarrow T)$ is the average linear thermal expansion coefficient over the temperature range $T_0$–$T$; $L_0$ is the sample length at $T_0$; $\Delta L$ is the length change when the temperature changes from $T_0$ to $T$; and the temperature change $\Delta T = T - T_0$. In our experiment, $T_0$ = 303.15 K and $\Delta L/L_0$ was obtained from Fig. 5. The calculated average linear thermal expansion coefficients of the NdCOB crystal are shown as dotted lines in Fig. 5.

Since the linear thermal expansion coefficient $\alpha$ is a symmetric second-rank tensor and temperature $T$ is a scalar, we can consider $\Delta L/L_0$ to be a symmetric second-rank tensor from the definition $\alpha = (\Delta L/L_0)(1/dT)$. Therefore the same discussion of symmetric second-rank tensors $[T_{ij}]$ mentioned above (Section 3.2) can be used to treat $[(\Delta L/L_0)_{ij}]$.

The mean values of the linear thermal expansion coefficients are $OX_1 = 8.5917 \times 10^{-6}\,K^{-1}$, $OX'_1 = 6.4885 \times 10^{-6}\,K^{-1}$, $OX_2 = 6.3727 \times 10^{-6}\,K^{-1}$, $OX_3 = 12.4358 \times 10^{-6}\,K^{-1}$ and $OX'_3 = 10.2554 \times 10^{-6}\,K^{-1}$. Using the method mentioned above we find the linear thermal expansion tensor to be given by

$$\alpha \times 10^{-6} = \begin{pmatrix} 6.8598 & 0 & 0.7544 \\ 0 & 6.3727 & 0 \\ 0.7544 & 0 & 12.0259 \end{pmatrix} K^{-1} \quad (11)$$

The components along the principal axes are 6.75189, 6.3727 and 12.13381 × $10^{-6}\,K^{-1}$, respectively. The rotation angle $\alpha$ is −16.28° (the negative sign indicates the principal axes are rotated clockwise around the $b$-axis) from the $c$ direction.

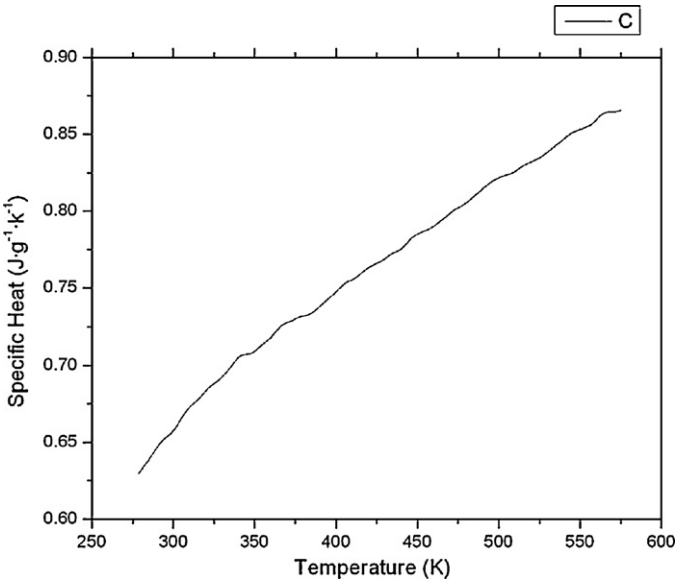


**Fig. 6.** Specific heat dependence of NdCOB on temperature.

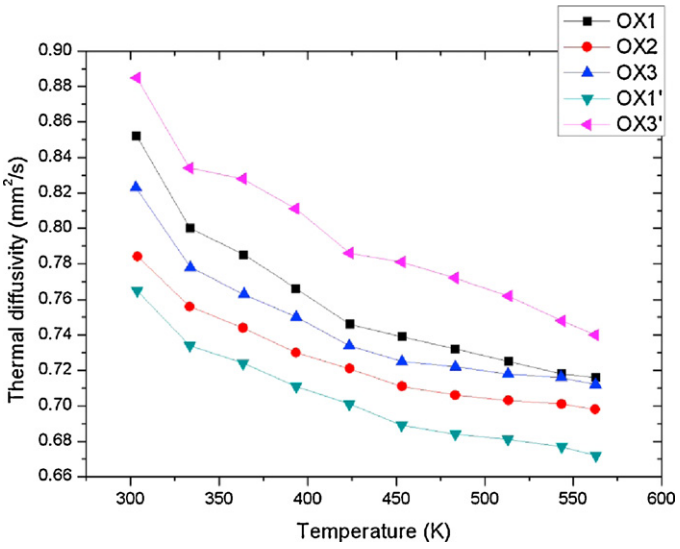


**Fig. 8.** Thermal diffusivity of NdCOB single crystal along $OX_1$, $OX_2$, $OX_3$, $OX_1'$ and $OX_3'$ directions.

The rotation angle can cause a phase mismatch for an incident laser beam when monoclinic crystals are used in nonlinear optics applications, which demand precise phase matching. As a consequence, phase mismatch will reduce optical–optical conversion efficiency in the nonlinear process. From Fig. 7, the angle $\theta$ between the principal axes and $[T_{ij}]$ does not remain constant but decreases with increasing temperature. The change in $\theta$ over the temperature range of 303.15–768.15 K is about 8.4°. Compared to the analogous change in $Er^{3+}$:$Yb^{3+}$:YCOB (15° over the temperature range of 303.15–873.15 K) [20], the rotation angle of NdCOB is almost half, which indicates that NdCOB crystals are more suitable for phase matching and increasing conversion efficiency.

### 3.4. Specific heat and thermal conductivity of NdCOB crystal

Fig. 6 displays the constant pressure specific heat versus temperature curve of the NdCOB crystal, measured by differential scanning calorimetry. It can be seen that the specific heat increases from 0.539 to 0.84 J $g^{-1}$ $K^{-1}$ as the temperature increases from 293.15 to 573.15 K.

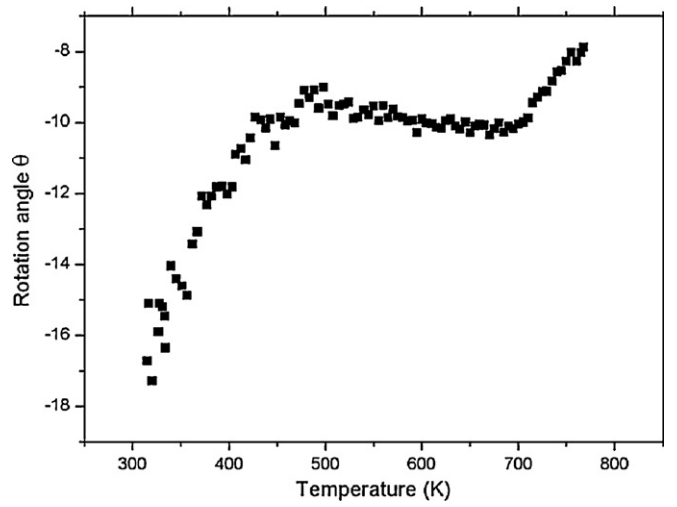


**Fig. 7.** Rotation angle of the principal axis from the crystallographic axis in NdCOB.

A least-squares to the curve gives the following equation with residual $R^2 = 0.99818$:

$$C_p = 0.08121 + 0.00128 \times T + 7391.50942 \times T^{-2} \quad (12)$$

The specific heat of NdCOB is as large as that of YCOB, a material that possesses a high damage threshold (~1 GW/$cm^{-2}$)[21]. So it can be inferred that NdCOB should have an analogously high damage threshold.

The value of the thermal conductivity of a laser crystal is of great importance from both a fundamental and a technical perspective. It can be calculated using the following equation:

$$k = \lambda \rho C_p \quad (13)$$

where $k$, $\lambda$, $\rho$ and $C_p$ denote the principal thermal conductivity, the thermal diffusion coefficient, the density and the specific heat of the crystal, respectively [22]. In our experiment, the thermal diffusion coefficients of the NdCOB crystal were measured directly over the temperature range of 303.15–562.15 K. The density of the crystal was measured to be about 3.62073 g $cm^{-3}$ using the buoyancy method at room temperature, 299.15 K. The density of the crystal was determined to be constant since the largest thermal expansion ratio along the principal axes is no larger than 0.5% over this temperature range. The thermal conductivity along the directions in which the thermal expansion was measured was calculated according to Eq. (13), and the data are shown in Figs. 8 and 9.

Fig. 8 shows the thermal diffusivity of NdCOB over the temperature range from 303.15 to 562.65 K at 30 K intervals between measured points. It can be seen that the thermal diffusivity along these directions in the crystal is anisotropic and decreases with increasing temperature.

The thermal conductivity $[k_{ij}]$ of a crystal is also a symmetric second-rank tensor. The principal axes of $[k_{ij}]$ can be found as discussed in Section 3.3. It can be seen that the NdCOB crystal possesses a weakly anisotropic thermal conductivity.

The thermal conductivity of NdCOB obtained along different directions, using the equation $k = \lambda \rho C_p$, is plotted in Fig. 9. At 303.35 K the thermal conductivity components of NdCOB are 2.0507, 1.88851, 1.97965, 1.84246 and 2.13047 W $m^{-1}$ $K^{-1}$ along the $OX_1$, $OX_2$, $OX_3$, $OX_1'$ and $OX_3'$ directions, respectively. The ther-

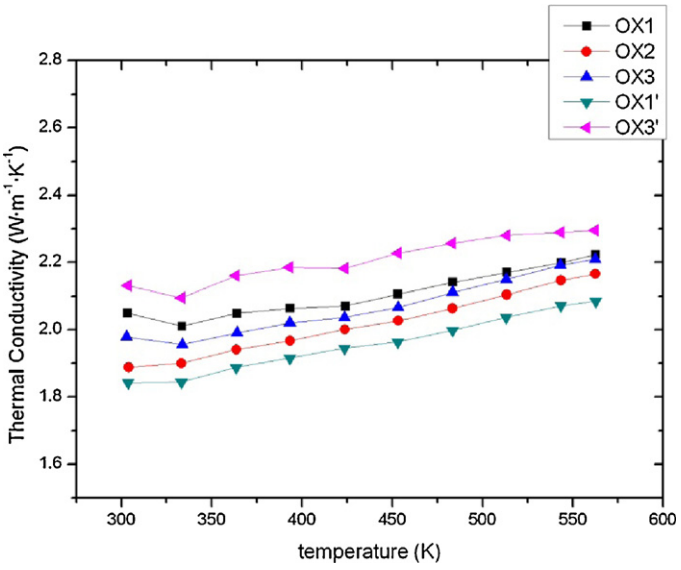


**Fig. 9.** Thermal conductivity of NdCOB single crystal along $OX_1$, $OX_2$, $OX_3$, $OX_1'$ and $OX_3'$ directions.

mal conductivity tensor is

$$k = \begin{pmatrix} 1.9642 & 0 & 0.1437 \\ 0 & 1.8885 & 0 \\ 0.1437 & 0 & 2.0374 \end{pmatrix} \text{W m}^{-1}\text{K}^{-1}$$

and the principal components of the tensor are 1.852512, 1.8885 and 2.149088 $\text{W m}^{-1}\text{K}^{-1}$. The rotation angle is −4.316° with respect to the *c* direction. A higher thermal conductivity will lead to a higher damage threshold. Compared to 2.0 $\text{W m}^{-1}\text{K}^{-1}$ for GdCOB [23], 3.01 $\text{W m}^{-1}\text{K}^{-1}$ for YCOB [24], 5.1 $\text{W m}^{-1}\text{K}^{-1}$ for Nd:$YVO_4$ [25] and 11.7 $\text{W m}^{-1}\text{K}^{-1}$ for Nd:$GdVO_4$ [26], NdCOB has a lower damage threshold when used in laser applications, especially at high power.

From the figure it is clear that the thermal conductivity increases abnormally with increasing temperature. This result differs from other monoclinic crystals, such as YCOB [27], Yb:Klu$(WO_4)_2$ [28] and $Lu_2SiO_5$ [29]. As reported before by Eucken [30], the temperature dependence of the thermal conductivity of a glassy material is quite dissimilar from that of a crystalline one. The thermal conductivity of glasses increases with increasing temperature, an effect that is consistent with the behavior of NdCOB. This phenomenon is probably due to the high structural disorder in NdCOB. Ilyukhin and Dzhurinskii [31] showed that, in a structural investigation of GdCOB, there might be some disorder that exists between calcium and gadolinium atoms in filling the two octahedral positions. Hence we can explain this abnormal result by assuming that the neodymium ions have replaced both gadolinium and calcium, which actually would increase the disorder in NdCOB.

## 4. Conclusions

A high-quality NdCOB crystal has been grown along the crystallographic *b*-axis using the Czochralski method. The crystal structure belongs to the monoclinic system with space group Cm; the unit-cell parameters are $a = 0.813$, $b = 1.606$, and $c = 0.359$ nm, and $\beta = 101.4°$. The measurements and calculations associated with evaluating a generalized symmetric second-rank tensor for the monoclinic crystal have been discussed in detail. The thermal properties of NdCOB were studied using single crystal samples. The principal coefficients of the thermal expansion tensor are $T_I = 6.75189 \times 10^{-6}\,\text{K}^{-1}$, $T_{II} = 6.3727 \times 10^{-6}\,\text{K}^{-1}$ and $T_{III} = 12.13381 \times 10^{-6}\,\text{K}^{-1}$ over the temperature range of 303.15–768.15 K. The specific heat of the crystal is fitted to Eq. (12) using the least-squares method. The principal thermal conductivity parameters are 1.9642, 1.8885 and 2.0374 $\text{W m}^{-1}\text{K}^{-1}$. These experimental results exhibit a weak anisotropy in the thermal expansion and thermal conductivity tensors. These characteristics are quite suitable for obtaining good quality crystal growth and for highly demanding laser applications.

## References

[1] J.Y. Wang, Z.S. Shao, J.Q. Wei, X.B. Hu, Y.G. Liu, B. Gong, G.M. Li, J.H. Lu, M. Guo, M.H. Jiang, Progress in Crystal Growth and Characterization of Materials, 2000, pp. 17–31.
[2] R. Norrestam, M. Nygren, J.O. Bovin, Chem. Mater. 4 (1992) 737.
[3] G. Aka, L. Bloch, J.M. Benitez, et al., in: S.A. Payne, C. Pollock (Eds.), OSA TOPS on Advanced Solid-State Lasers, vol. I, 1996, pp. 336–340.
[4] M. Iwai, T. Kobayashi, H. Furuya, Y. Mori, T. Sasaki, Jpn. J. Appl. Phys. 36 (1997) 276–279.
[5] M. Yoshimura, T. Kobayashi, H. Furuya, et al., Yttrium Calcium Oxyborate $YCa_4O(BO_3)_3$ for Blue and UV Generation, CWG2, CLEO'98, 1998, p. 270.
[6] Z.D. Luo, A.D. Jiang, Y.C. Huang, M.W. Qiu, Sci. China Ser. A 34 (1991) 6.
[7] N. Hiroshi, N. Masahiro, S. Takashi, S. Hiroyuki, T. Hiroaki, S. Tadashi, J. Alloys Compd. 408–412 (2006) 582–585.
[8] T. Hiroaki, N. Hiroshi, I. Shintaro, S. Hiroyuki, N. Takashi, O. Soichiro, S. Tadashi, J. Alloys Compd. 408–412 (2006) 474–479.
[9] E. Brzozowski, W. Soluch, Electron. Lett. 44 (1) (2008).
[10] T. Karaki, M. Adachi, Y. Kuniyoshi, J. Electroceram. 21 (2007) 823–826.
[11] Y.G. Yu, J.Y. Wang, H.J. Zhang, H.H. Yu, Z.P. Wang, M.H. Jiang, H.R. Xia, R.I. Boughton, J. Opt. Soc. Am. B 25 (6) (2008) 995–1001.
[12] Y.M. Yu, J.J. Ju, M. Cha, J. Cryst. Growth 229 (2001) 175–178.
[13] H. Nakao, M. Nishida, T. Shikida, H. Shimizu, H. Takeda, T. Shiosaki, J. Alloys Compd. 408–412 (2006) 582–585.
[14] W.B. Hou, D. Xu, D.R. Yuan, M.G. Liu, N. Zhang, X.T. Tao, S.Y. Sun, M.H. Jiang, Cryst. Res. Technol. 29 (7) (1994) 939–944.
[15] D. Xu, K.C. Zhang, L.H. Zhang, Science and Technology of Crystal Growth, Science Press, Beijing, 1997 (in Chinese).
[16] Q. Ye, B.H.T. Chai, J. Cryst. Growth 197 (1999) 228–235.
[17] J.F. Nye, Physical Properties of Crystals: Their Representation by Tensors and Matrices, Clarendon Press, Oxford, 1985.
[18] R.S. Krishnan, R. Srinivasan, S. Devanarayanan, Thermal Expansion of Crystals, Pergamon Press, Oxford, 1979.
[19] C.Y. Ho, T.H.K. Barron, A. Cezairliyan, P.S. Gaal, in: R.E. Taylor (Ed.), Thermal Expansion of Solids, ASM International, Materials Park, 1998.
[20] W.W. Ge, H.J. Zhang, J.Y. Wang, M.H. Jiang, et al., J. Appl. Cryst. 40 (2007) 125–132.
[21] W. Zwicher et al., AD A119457, 1983.
[22] W.J. Parker, R.J. Jenkins, C.P. Butler, G.L. Abbott, J. Appl. Phys. 32 (1961) 1679–1684.
[23] F. Mougel, A. Kahn-Harari, G. Aka, D. Pelenc, J. Mater. Chem. 8 (1998) 1619.
[24] Q. Ye, L. Shah, J. Eichenholz, D. Hammons, R. Peale, M. Richardson, A. Chin, B.H.T. Chai, Opt. Commun. 164 (1999) 33.
[25] P.A. Studenikin, A.I. Zagumennyi, D. Yu, P.A. Zavartsev, I.A. Popov, Shcherbakov, Quantum Electron. 25 (1995) 1162.
[26] B.H.T. Chai, G. Loutts, J. Lefaucheur, et al., OSA Proceedings of the Advanced Solid-State Lasers, vol. 20, Optical Society of America, Washington, DC, 1994, p. 41.
[27] J. Luo, S.J. Fan, H.Q. Xie, K.C. Xiao, S.X. Qian, Z.W. Zhong, G.X. Qian, R.Y. Sun, J.Y. Xu, Cryst. Res. Technol. 36 (2001) 1215–1221.
[28] J.X. Zhang, K.P. Wang, J.Y. Wang, H.J. Zhang, et al., Appl. Phys. Lett. 87 (2005) 061104.
[29] H.J. Cong, H.J. Zhang, J.Y. Wang, et al., J. Appl. Cryst. 42 (2009) 284–294.
[30] A. Eucken, Über die Temperaturabhängigkeit der Wärmeleit-fähigkeit fester Nichtmetalle, Annalen Den Physik 339 (2) (1911) 185–221.
[31] B. Ilyukhin, B.F. Dzhurinskii, Russ. J. Inorg. Chem. 38 (1993) 847.